

Thickness effect of a Ge interlayer on the formation of nickel silicides

최철중,¹ 장성용,² 이성재,³ 옥영우,⁴ 성태연⁴

¹*IT Convergence Technology Research Division, Electronics and Telecommunications Research Institute (ETRI)*

²*Materials Engineering Group, Korea Electric Power Research Institute (KEPRI)*

³*Department of Physics, Hanyang University*

⁴*Department of Materials Science and Engineering, Korea University*

Introduction

Because of the ever-increasing demand for scaling down complementary metal-oxide-semiconductor (CMOS) devices, a silicide process has become an essential technology for high speed and performance logic in ultra large scale integrated (ULSI) circuits. Among all silicides, CoSi₂ has been most commonly used due to its low electrical resistance and various application fields.¹ However, it suffers from large Si consumption and irregular interfaces between CoSi₂ and Si-substrate. Recently, NiSi has been regarded as a promising candidate for the development of high performance CMOS devices.² NiSi has superior properties, such as low resistivity (14~20 Ωcm), line-width independent sheet resistance, no bridging failure, and low barrier height of contacts between the silicide and n- or p-type Si.³ In addition, Si consumption during silicidation is the smallest among all metal silicides, which is an attractive feature for next generation CMOS devices. However, a major concern with NiSi is phase transformation of NiSi into NiSi₂ (resistivity : 35~50 Ωcm) at relatively low temperatures (~700°C).⁴ It should be noted that after silicidation, a high temperature annealing process is required for the reflow of interlayer dielectrics (ILD) such as borophosphosilicate glass (BPSG). Such a high temperature process is typically performed above 850°C, which is much higher than the nucleation temperature of NiSi₂. In this work, we have investigated the effect of a Ge interlayer on the electrical and structural properties of Ni-silicides. It is shown that the NiSi₂ nucleation temperature strongly depends on the thickness of Ge interlayers. It is also shown that Ge segregation enhances the

agglomeration of Ni-silicides.

Experiment

After removing the native oxide using dilute HF solution, 2 and 5 nm-thick Ge films were electron-beam-evaporated on (100) Si-substrates, followed by the sequential evaporation of 30 nm-thick Ni films without breaking vacuum. For Ni silicidation reactions, the samples were rapid thermal annealed at temperatures in the range 400 - 900 C for 30 s in N₂ ambient. In order to remove the unreacted metal, the rapid-thermal-annealed samples were treated by a mixture of H₂SO₄ and H₂O₂ solutions. To investigate the effect of Ge interlayers on their structural and electrical properties, the sample without a Ge interlayer was also prepared at the same conditions. For convenience, Ni(30 nm)/Ge(2 nm)/Si, Ni(30 nm)/Ge(5 nm)/Si, and Ni(30 nm)/Si samples are referred to here as '2 nm-interlayer', '5 nm-interlayer', and 'no-interlayer' samples, respectively.

Results and discussion

Fig. 1 shows GXRD plots of the samples with and without the interlayers as a function of the temperature. For the no-interlayer samples, only an orthorhombic NiSi phase is formed, when annealed at temperatures below 650°C. However, a new phase (*e.g.*, NiSi₂ phase with a CaF₂ type cubic structure) appears at 700°C, and then NiSi is completely transformed into NiSi₂ when annealed at 750°C. It is worth noting that the NiSi-to-NiSi₂ transformation behavior of the 2 nm and 5 nm-interlayer samples is different from that of the no-interlayer sample. In other words, the temperatures for the nucleation of NiSi₂ in the samples with the interlayers are increased by higher than 150°C. This indicates that the use of the Ge interlayer effectively expands the RTA processing window for the formation of a NiSi film.

Fig. 2 exhibits cross-sectional bright field (BF) TEM images obtained from the samples with the interlayers annealed at 500°C for 30 s. For both the samples, there exists an additional thin layer (indicated by the arrow) at the interface between the NiSi film and the Si substrate. EDX analyses (not shown) demonstrated that these layers contain a mixture of Ni, Si, and Ge, implying the formation of ternary NiSi_{1-x}Ge_x. High-resolution electron microscopy (HREM) images (the insets of Fig. 2) show that for the 2 nm-interlayer sample [Fig. 2(a)],

the crystalline $\text{NiSi}_{1-x}\text{Ge}_x$ layer is thinner than that of the 5 nm-interlayer sample [Fig. 2(b)]. In addition, for the 2 nm-interlayer sample, the $\text{NiSi}_{1-x}\text{Ge}_x$ layer (~ 4 nm thick) is relatively uniform, while for the 5 nm-interlayer sample, the ternary layer (~ 8 nm thick) is irregular with thermal grooves.

In order to investigate the distribution of elements in the samples with the interlayers annealed at 500°C for 30 s, cross sectional STEM-EDX mapping for Ni, Si, and Ge atoms was performed (Fig. 3). As shown in the TEM results (Fig. 2), the mapping of Ni and Si indicates the formation of NiSi films [Figs. 3(b, c, f, and g)]. However, Ge atoms are mostly present at the surface and the NiSi/Si substrate interface regions. This indicates that a large amount of Ge is outdiffused to the surface region through the NiSi film. Such outdiffusion behavior could be explained in terms of the difference in the surface tension of the elements in the present sample.⁵

Fig. 4 shows cross-sectional STEM Z-contrast images and corresponding EDX compositional maps for Ni, Si, and Ge atoms in the samples with the interlayers after annealing at 850°C for 30 s. For both the samples, the silicide films become severely agglomerated. EDX point analyses (not shown) showed that the silicide films of the 2 nm and 5 nm-interlayer samples are NiSi_2 and NiSi phases, respectively. Furthermore, the STEM and EDX mapping results show that for both the samples, $\text{Si}_{1-x}\text{Ge}_x$ layers [indicated by the arrows in Figs. 4(a), and 4(e)] are formed in-between the agglomerated silicides. The $\text{Si}_{1-x}\text{Ge}_x$ layer of the 5 nm-interlayer sample is thicker than that of the 2 nm-interlayer one. For the 5 nm-interlayer sample, Ge atoms are also present in-between the NiSi film and Si-substrate [indicated by arrow in Fig. 4(h)]. However, for the 2 nm-interlayer sample, there is no evidence for the presence of Ge atoms at the interface region between the silicide/Si substrate. This indicates that there exist $\text{NiSi}_{1-x}\text{Ge}_x$ phase in the 5 nm-interlayer sample, but not in the 2 nm-interlayer sample.

According to the classical theory of the nucleation, activation energy required for the transformation of NiSi_2 from $\text{NiSi}_{1-x}\text{Ge}_x$ is higher than that from pure NiSi, because of lower free-energy level in $\text{NiSi}_{1-x}\text{Ge}_x$ driven by increasing the entropy of mixing.⁶ From the TEM and STEM-EDX results, it is evident that the ternary $\text{NiSi}_{1-x}\text{Ge}_x$ and NiSi films are formed simultaneously during low temperature annealing. As the temperature increases, Ge outdiffuses from the $\text{NiSi}_{1-x}\text{Ge}_x$ more readily and consequently segregates at the surface region, since Ni-Si bonding has

a lower heat formation energy compared with that of Ni-Ge bonding.⁷ Such Ge outdiffusion behavior causes the thickness reduction of the NiSi_{1-x}Ge_x layer. The presence of the NiSi_{1-x}Ge_x layer in-between the NiSi film and the Si-substrate hinders Si supply (or Ni diffusion) required for the NiSi₂ nucleation. This causes the slowing down of phase transformation from NiSi to NiSi₂. Thus, during annealing at high temperatures, a thick NiSi_{1-x}Ge_x layer is more effective in delaying NiSi₂ nucleation, compared to a thin NiSi_{1-x}Ge_x layer. Furthermore, the segregated Ge atoms react with Si and participate in the formation of Si_{1-x}Ge_x layer at the surface region in order to minimize surface energy.⁸

Conclusion

We investigated the Ge interlayer thickness dependence on the electrical and micro-structural properties of Ni-silicides as a function of the rapid-thermal-annealing temperature. For the sample without the interlayer, NiSi transformed into NiSi₂ at 700°C. For the samples the interlayers, however, the NiSi₂ nucleation temperatures increased up to 850 and 900°C due to the presence of NiSi_{1-x}Ge_x ternary layers formed in-between the NiSi films and Si-substrates.

Reference

- [1] K. Maex, *Mater. Sci. Eng.*, R11, 53 (1993).
- [2] T. Morimoto et al., *Tech. Dig. Int. Electron Devices Meet.*, 653 (1991).
- [3] C-J. Choi et al., *Jpn. J. Appl. Phys.*, 41, 1969 (2002).
- [4] C-J. Choi et al., *J. Electrochem. Soc.*, 149, G512 (2002).
- [5] F.L. Williams et al., *Surf. Sci.*, 45, 377 (1974).
- [6] S.-L. Zhang, *Microelectron. Eng.*, 70, 174 (2003).
- [7] J.S. Luo et al., *J. Appl. Phys.*, 82, 3621 (1997).
- [8] P.C. Kerlres et al., *Phys. Rev. Lett.*, 63, 1164 (1989).

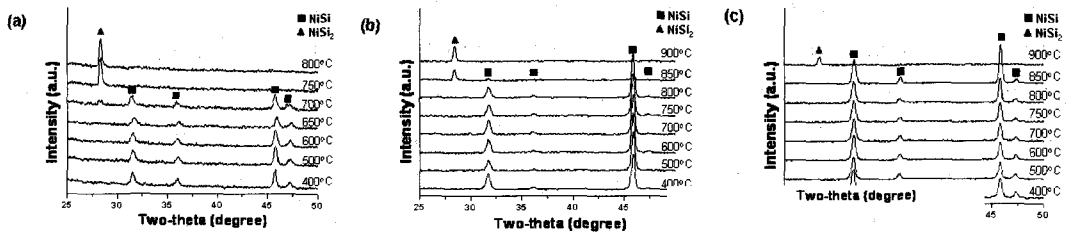


Fig. 1. GXR D plots of the samples (a) without the interlayer, and with (b) the 2 nm-thick and (c) 5 nm-thick interlayers as a function of the rapid-thermal-annealing temperature.

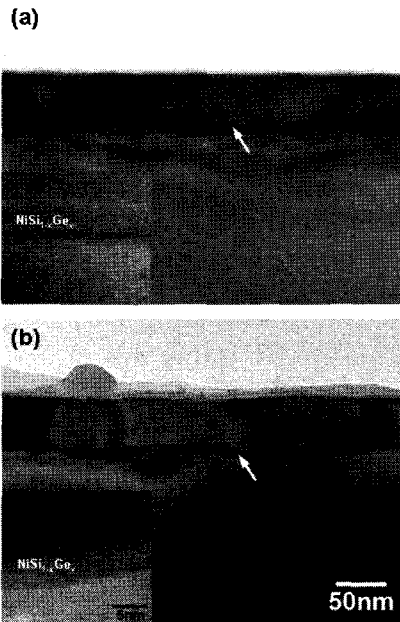


Fig. 2. Cross-sectional BF TEM images taken from (a) 2 nm-interlayer and (b) 5 nm-interlayer samples after annealing at 500°C for 30 s.

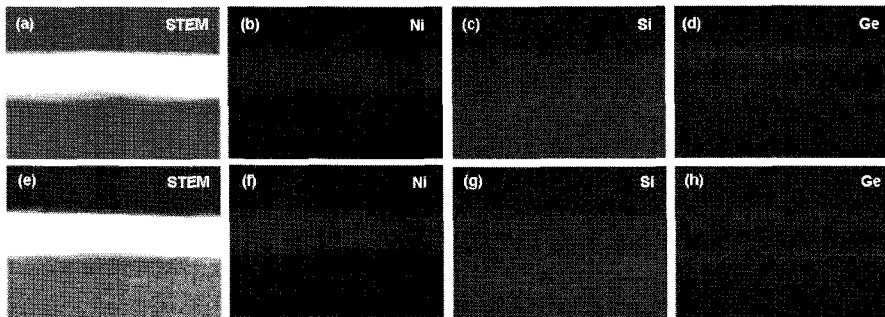


Fig. 3. (a) and (e) Cross sectional STEM Z-contrast images, and corresponding STE-EDX maps for (b) and (f) Ni, (c) and (g) Si, and (d) and (h) Ge atoms obtained from the samples with the 2 nm and 5 nm-interlayers after annealing at 500 °C for 30 s, respectively.

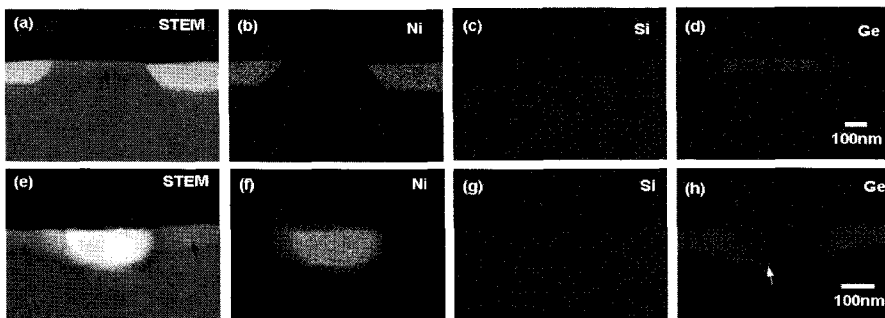


Fig. 4. (a) and (e) Cross sectional STEM Z-contrast images, and corresponding STE-EDX maps for (b) and (f) Ni, (c) and (g) Si, and (d) and (h) Ge atoms obtained from the samples with the 2 nm and 5 nm-interlayers after annealing at 850°C for 30 s, respectively.

성명	Page,구분
권기현	92, 재포4
권희석	37, S3
권희석	65, 의포10
김규현	33, S3
	94, 재포5
	101, 재포7
김동환	104, 재포8
김동희	68, 의포11
김영수	68, 의포11
김상우	101, 재포7
김영민	84, 재포2
김원	38, S3
김윤중	65, 의포10
	84, 재포2
	90, 재포3
	92, 재포4
김은수	71, 의포12
김진규	65, 의포10
	90, 재포3
	92, 재포4
김한성	33, S3
	101, 재포7
김현길	96, 재포6
김호정	38, S3
박경수	43, S3
박상운	96, 재포6
박수진	65, 의포10
박정희	33, S3
박종봉	43, S3
박주철	43, S3
박창현	68, 의포11
백태선	38, S3
성태연	108, 재포9
손성규	38, S3
송세안	43, S3
신동훈	68, 의포11
안재평	33, S3
	94, 재포5
	101, 재포7
	104, 재포8
엄창섭	68, 의포11
오윤식	65, 의포10
옥영우	108, 재포9
옥정현	65, 의포10
윤상원	33, S3
	94, 재포5
	101, 재포7
	104, 재포8
이경환	71, 의포12
이귀영	68, 의포11
이명호	96, 재포6
이상은	71, 의포12

성명	Page,구분
이상희	65, 의포10
	90, 재포3
이성재	108, 재포9
이순영	38, S3
이재철	94, 재포5
이주연	65, 의포10
이준호	43, S3
이지영	65, 의포10
이현주	104, 재포8
장병수	68, 의포11
장성용	108, 재포9
정용환	96, 재포6
정종만	65, 의포10
	92, 재포4
재정호	13, S1
최병권	96, 재포6
최철중	108, 재포9
한성식	29, S3
Chul Jong Yoon	49, 의포1
Dr. Bernd Altrichter	24, S2
Eun Soo Kim	75, 의포13
Eun-Ah Park	55, 의포5
Gabriele Murer	24, S2
Hwang Ki-Ju	51, 의포2
Im Joo Rhyu	32, S3
InSun Kim	51, 의포2
	52, 의포3
J. -H. Cho	81, 재포1
J. -Y. Yun	81, 재포1
Jae-Young Choi	55, 의포5
Jong-Gu Park	57, 의포6
	59, 의포7
Jung-Hyun Ryu	55, 의포5
Ki Woo Kim	49, 의포1
Ko Kyung Nam	75, 의포13
Kyung-Hwun Chung	53, 의포4
Kyung-Whan Lee	75, 의포13
Min-Hee Yu	61, 의포8
	63, 의포9
Ms. Efrat M Ras	21, S2
Myung-Jin Moon	53, 의포4
	55, 의포5
	57, 의포6
	59, 의포7
	61, 의포8
	63, 의포9
S. -H. Lim	81, 재포1
Sang-Eun Lee	75, 의포13
William Neijssen	26, S2
Y. -D. Tark	81, 재포1
Yung Doug SUH	15, S1

S1 : Session I

S2 : Session II

S3 : Session III

의포 : 의생활 포스터

재포 : 재료 포스터